A pH-differential Dual-Electrolyte Microfluidic Reactor for Electrochemical Reduction of CO_2

Xu Lu [1], Dennis Y.C. Leung [1,*], Huizhi Wang [2], M. Mercedes Maroto-Valer [2], Jin Xuan [2,*]

[1] Department of Mechanical Engineering, The University of Hong Kong, Pokfulam, Hong Kong

[2] Centre for Innovation in Carbon Capture and Storage (CICCS), School of Engineering and Physical Sciences, Heriot-Watt University, Edinburgh, U.K.

[*] Corresponding authors, Tel.: +852 2859 7911, fax: +852 2858 5415, email: ycleng@hku.hk (D.Y.C. Leung); Tel: +44 (0) 131 451 3293; Fax: +44 (0)131 451 3129, email: j.xuan@hw.ac.uk (J. Xuan)

Abstract

CO_2 can be converted to useful fuels by electrochemical processes. As an effective strategy to address greenhouse effect and energy storage shortage, electrochemical reduction of CO_2 still needs major improvements on its efficiency and reactivity. Microfluidics provides the possibility to enhance the electrochemical performance, but its virtual interface is lack of development. This work demonstrates a dual electrolyte microfluidic reactor (DEMR) that improves the thermodynamic property and raises the electrochemical performance based on a laminar flow membrane-less architecture. Freed from hindrances of membrane structure and thermodynamic limitation, DEMR could bring in 6 times higher reactivity and draws electrode potentials closer to the equilibrium status (corresponding to less electrode overpotentials). The cathode potential was reduced from -2.1V to -0.82V and the anode potential dropped from 1.7V to 1V. During the conversion of CO_2, the peak Faradaic and energetic efficiencies were recorded as high as 95.6% at 143 mA/cm^2 and 48.5% at 62 mA/cm^2, respectively, and hence, facilitating future potential for larger-scale applications.

Keywords

CO_2 utilization

Energy storage

Electrochemistry

Dual electrolyte

Microfluidics

1. Introduction

Issues related to carbon dioxide (CO_2) emission become increasingly important. Instead of CO_2 capture and sequestration, electrochemical conversion of CO_2 into usable fuels is an important option to provide a solution towards a carbon-neutral energy conversion.

Many research efforts on electrochemical reduction of CO_2, and specifically on the development of electrode materials, have focused on increasing the reactivity and reducing the overpotential for a higher Faradaic efficiency. Various noble metal-based catalysts and different compositions have been tested with low electrical resistances in a three-electrode system[1, 2] and the synthesis of catalysts have demonstrated high turnover numbers as high as 350 h^{-1}[3]. Studies on catalyst structures, especially gas diffusion layers (GDLs), have been conducted to enhance the three-phase interaction and hence a larger active site area[4, 5]. The implementation of a gas diffusion electrode (GDE) with high porosity and specific surface in a DEMR help relieve the constraint from the effective electrolyte conductivity and electro-active site thickness limitations. In general, an electrode of an electrolytic cell comprises a substrate and a catalyst layer (CL), serving multiple functions in electrochemical reduction of CO_2 to formic acid, such

as absorbing gaseous CO_2, transporting CO_2 from substrate to the CL, providing an active reaction site for catalyst(s) adhered on its surface, deliver formic acid from the CL into the electrolyte, and conducting protons and electrons with low resistance. At early stage, substantial attempts on developing electrodes with planar and mesh structures[6] were conducted, but outcomes were mostly unsatisfactory. GDEs, which create effective three-phase interfaces for gaseous reactants, electrodes and electrolytes, have been developed rapidly and are regarded as an effective solution towards low gaseous feed transfer rate and poor cell performance[7, 8]. A GDE usually comprises of a conventional catalyst layer, where carbon black is usually utilized to support catalyst particles, and a GDL[9]. GDL is usually made from porous materials and dense array of carbon fibers, whose high surface area would facilitate CO_2 transport and reduction. Two common examples are non-woven carbon paper and woven fabric carbon cloth, enhancing the interfacial area within the material of the electrode and the three-phase boundary. In addition to providing mechanical support and protection from corrosion or erosion, GDEs also perform other multiple roles including the pathway of CO_2 and electrolyte diffusion, intermediate of proton and electron transfer, passage for by-product removal for the purpose of preventing cathode flooding, medium of heat transfer. Studies of GDEs on CO_2 to formic acid conversion cell have been conducted by many researchers. Experiment with Pb-coated GDEs shows high reaction rate, high current density, high Faradaic efficiency ($\approx$95%) and reasonable applied potential[10]. Another high performance catalyst, Ru-Pd alloy particles, has been incorporated with GDEs[11] too, whose competitiveness was revealed by 90% current efficiency at -1.1 V vs. SCE and 80 mA/cm^2. Cu- and Zn- phthalocyanines have been coated and tested on GDEs, yielding formic acid at high current densities (100 mA/cm^2)[12]. The issue related to CO_2

solubility could also be relieved by GDE as the gaseous reactant molecules would diffuse through the porous reactive site with large geometric contact area[13].

More recently, multi-walled nanotubes and cobalt tetra-amino phthalocyanine composite modified electrodes were reported in literatures to further boost the catalysis process in terms of reactivity. Besides, the possibility of implementing ionic liquids[14-17] and organic electrolytes[18] [19, 20] as co-catalysts have been demonstrated to be able to improve the electrochemical performance and suppress side reactions. Although the above-mentioned methods have achieved slight catalyst degradations and low kinetic losses, electrode potentials have remained high and electrochemical reduction of CO_2 can hardly leap forward due to the thermodynamic limitation.

The aim of breaking the thermodynamic barrier has motivated a pH differential technique. It was reported that the overall cell and individual electrode potentials could be altered for better electrochemical performance by adjusting electrolyte pH conditions[21]. Although some researchers, including our group, have implemented this strategy in fuel cells and flow batteries with raised open-circuited voltages (OCV) and peak power densities[22], its application to electrolysis process, such as CO_2 electrochemical reduction, remains unexplored. A pH above 6 would affect the intrinsic kinetics of CO_2 to formic acid conversion because of the limited CO_2 mass transfer rate. pH would also alter the forms of products and high concentration of formic acid would not be formed in case of neutral or base condition (pK_a = 3.8 at 298 K)[23].

Theoretically, electrolyte pH adjustment would significantly lower electrode potentials and benefit CO_2 reduction by pairing the cathode with acid and the anode with alkaline electrolytes. Yet, most electrochemical reactors have been designed and developed based on polymer membrane structure[24, 25], which suffers from high cost, low interphase contact area, flooding

problem, and poor durability as an acid-alkaline separator. More recently, a state-of-the-art concept of microfluidic reactor has been reported[26, 27], using laminar electrolyte streams with distinctive behaviors to separate the cathode and anode. Microfluidics offers a virtual but effective layer to replace the conventional membrane, providing an ultimate solution towards some of the limitations of macroscale devices. Microfluidic electrochemical reactors soon spread widely in various applications such as quantitative detection of biological indicators[28, 29], synthesis of oxidation products[30], and wastewater treatment[31].

More specifically, researchers have shown the power of microfluidics to enhance the performance of CO_2 electrochemical reduction systems. By employing the microfluidic electrolyte flow, the water management issues at the electrode and membrane was eliminated. Additionally, continuous flow operation and individual electrode analysis becomes possible, making microfluidics an ideal electrochemical analysis platform. Multiple purposes were also well developed, including CO_2 sequestration[32], synthesis of gaseous fuels[33], CO_2 dissolution in physical solvents[34], and numerical analysis on intrinsic electrochemistry[35].

Despite these noticeable merits and achievements, breakthroughs of microfluidics on the electrochemical conversion of CO_2 to fuels could barely be found and it appears that the virtual layer is the key to facilitate further advancement. Microfluidics enables the operation conditions (e.g. electrolyte composition and pH) in a more flexible manner. The study by Whipple et al. [36] tested several electro-catalysts and the effects of electrolyte pH on the cell efficiency, revealing that cell operating at pH = 4 resulted in a significant improvement of cell performance, i.e. Faradaic and energetic efficiencies could achieve 89 and 45%, respectively, at current density of 100 mA cm^{-2}. These results pointed to the possibility that the thermodynamic constrains could be eliminated to some extent by microfluidics, because the membraneless nature could realize

individual tailoring of the composition of the anolyte and catholyte, thus allowing the kinetics and thermodynamic at the anode and cathode to be independently optimized[37]. Usually, in a membrane-based electrochemical system, the cell would be operated either on under acidic or alkaline media. In a microfluidic reactor, on the other hand, mixed-media operation could be achievable regardless of the membrane stability, i.e. one electrode in acidic media and another in alkaline conditions. Certain combinations of anode and cathode stream composition will result in very low on-set voltages, while other combinations may lead to high potentials as a result of the pH dependence of standard electrode potentials, which would be respectively favorable for CO_2 electrochemical reduction [37].

Accordingly, we report a dual electrolyte microfluidic reactor (DEMR) converting CO_2 into formic acid. Formic acid is selected as the target product because of its role as a common energy storage medium[38-40] and commercialization prospect[41, 42]. To optimize the reactor performance, our research covers electrode material selection, catalyst preparation, and pH optimization for anolyte and catholyte. By breaking the thermodynamic barrier, both reactivity and Faradaic efficiency of the system are enhanced, revealing a new solution towards greenhouse gas mitigation and energy storage shortage issues.

2. Methodology

2.1 Thermodynamic design

The major reactions under dual electrolyte arrangement in our DEMR are provided in Eq. 1, 2 and 3.

Cathode reaction (acid):

$$CO_2 + 2H^+ + 2e^- \rightarrow HCOOH \quad (1)$$

$$2H^+ + 2e^- \rightarrow H_2 \text{ (undesired)} \quad (2)$$

Anode reaction (alkaline):

$$2OH^- \rightarrow \frac{1}{2}O_2 + H_2O + 2e^- \quad (3)$$

The equilibrium potentials of the cathode reaction, $E_{cathode}$, can be calculated from Eq. 4 based on Nernst equation[43]:

$$E_{cathode} = {E_{cathode\ @\ pH=0}}^0 - \frac{RT}{2F} \cdot \ln\left(\frac{1+\frac{K_1}{[H^+]}\cdot\left(1+\frac{K_2}{[H^+]}\right)}{1+\frac{K_3}{[H^+]}} \cdot \frac{1}{[H^+]^2}\right) \quad (4)$$

where

R: the universal gas constant $8.314\ JK^{-1}mol^{-1}$,

T: temperature (298K),

F: Faraday constant ($96485\ Cmol^{-1}$),

K_1: the equilibrium constant between CO_2 and ${HCO_3}^-$ ($K_1 = e^{-pK_1} = e^{-6.39}$)[43],

K_2: the equilibrium constant between CO_2 and ${CO_3}^{2-}$ ($K_2 = e^{-pK_2} = e^{-10.32}$)[43],

K_3: the equilibrium constant between CO_2 and HCOOH ($K_3 = e^{-pK_3} = e^{-3.75}$)[43],

$K_i = e^{-pK_i}$,

${E_{cathode\ @\ pH=0}}^0$: standard electrode potential at pH=0 recorded in 10 mM formate and 10 mM CO_2 at 310K (-0.042V)[43],

$[H^+] = 10^{-pH}$.

Fig. 1 shows the Pourbaix diagrams of three dominant reactions in a CO_2 reduction system, i.e. CO_2 to formic acid reaction, undesirable hydrogen evolution reaction (HER), and anode oxygen evolution reaction. Corresponding Nernst potentials of each reactions are plotted against pH values[44]. As can be observed, the individual potentials of the oxygen and hydrogen electrodes

drop linearly with elevated pHs, whereas the CO_2 reduction potentials would be reduced at lowered pHs, demonstrating the thermodynamic foundation of a DEMR.

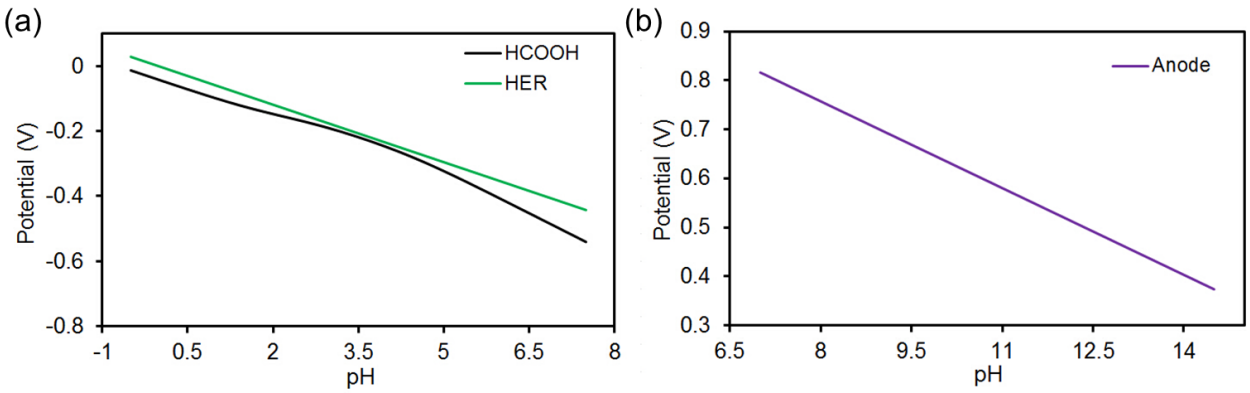

Fig. 1. Pourbaix diagrams of (a) CO_2 to HCOOH conversion (cathode reaction) and HER; and (b) oxygen evolution reaction (anode reaction).

2.2 Catalyst preparation

Commercially available catalysts (Johnson Matthey) supported by carbon paper were used as electrodes and Nafion (DuPont) solution was used as the catalyst binder. Different types of catalysts (i.e. Pd, PtRu, PtIr, Sn, Pt black, Pb) were used as mentioned in the catalyst selection section. Catalyst inks were prepared by sonicating mixtures of 28 mg catalyst, 126 µL of 10 wt % Nafion solution to achieve 30:1 catalyst to Nafion ratio, and 2800 µL of isopropyl alcohol for 1 h. The ink was then scattered onto a PTFE-hydrophobized gas diffusion carbon paper (HCP120, Hesen) with sizes 2.5 cm (L) × 1.1 cm (W) by spray gun. Measuring the net weight increase of carbon paper before and after spraying, the catalyst loading on the electrodes was 5 mg/cm^2.

2.3 Cell fabrication

The electrodes were housed between two 0.05-cm-thick Poly(vinyl chloride) (PVC) sheets as embedding plates. Two silver plates were used as current collectors. Each of the embedding plates were machined with a 0.2 cm (W) ×0.5 cm (L) window as reaction area. Two 0.01-cm-

thick PVC sheets were used to separate the electrodes and create identical anolyte and catholyte channels of 0.2 cm (W) ×7.5 cm (L), between which another 0.01-cm-thick PVC sheet with a 0.2 cm (W) ×0.5 cm (L) window was sandwiched in-between, indicated as 'insulating separator' in Fig. 2. The insulating separator is used to form the catholyte and anolyte interactive and contact area. A 5 cm (L) × 1 cm (W) × 0.5 cm (H) chamber was machined to act as the CO_2 reservoir for the cathode side. All layered components were fabricated using CO_2 laser ablation system (VLS 2.30, Universal Laser System) and clamped together by binder clips (Highmark), as shown in Fig. 2.

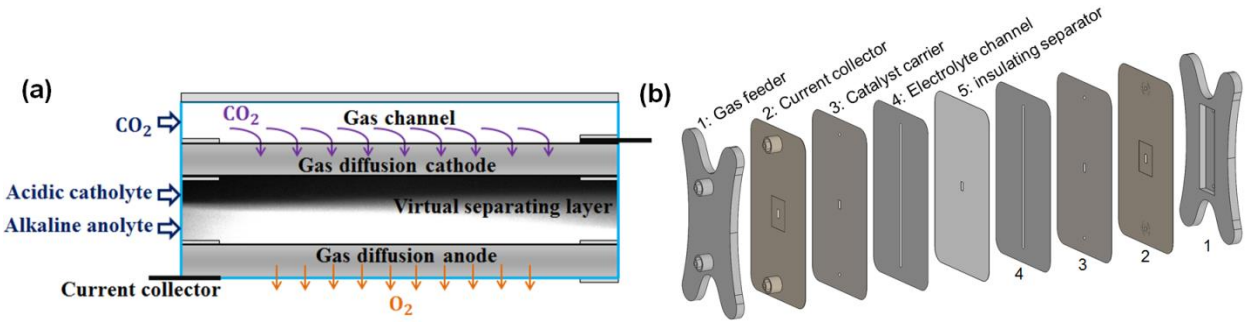

Fig. 2. Demonstration of the microfluidic reactor. (a) Schematic diagram of a DEMR; and (b) Component configuration (N.B. the virtual separating layer is identified by fluorescein microscopy).

2.4 Electrochemistry

Electrochemical tests were conducted by holding the cell at constant potentials by an electrochemical station (CHI600E, CHInstruments, Inc) with a sampling frequency of 250 Hz. The measurement and record of each data point took a total of 200 seconds. The first 100 seconds was the stabilizing phase, followed by the 100-second steady state. Each data point was collected by averaging the integration of the 100-second steady-state current data to eliminate transient artifacts. Controlled by a mass flow controller (GFC17, Aalborg), gaseous CO_2 (≥ 99.5%

purity, Linde) was fed into the cathode chamber at a flow rate of 80 mL/min and migrated through the GDLs to the catalyst surfaces. Electrolytes stored in syringe tubes were driven by syringe pumps (LSP02-1B, Longer Pump) at a flow rate of 500 $\mu L/min$ and continuously guided through the microchannels by plastic tubes. The electrolytes were not recirculated and the sringe tubes were refilled upon electrolyte depletion to restart the experiment. Individual potentials of anode and cathode were recorded with digital multi-meters (Fluke) connected between each electrode and an external Ag/AgCl reference electrode in the exit electrolyte stream. Current and power densities were calculated using the exposed surface area of the electrodes (i.e. 0.1 cm^2).

In terms of the cations/anions selection, there exists an inter-conversion amongst CO_3^{2-}, HCO_3^- and $CO_2(aq)$[45-47], where high concentration of CO_3^{2-} would be beneficial to the chemical kinetics of the HCO_3^-evolution but lower the selectivity of formic acid generation[23]. Under slight base condition, the reaction: $HCO_3^- + OH^- \rightarrow CO_3^{2-} + H_2O$ would decrease the pH and hence deplete $CO_2(aq)$ as well. Because of the complexity with respect to the inter-conversion and the fact that other anions, such as $Cl^-$and Br^-, would bring in the risk of electrolysis towards poisonous oxidants, SO_4^{2-} is used in this study. It should also be noted that K^+ was selected as the cation because the cathode potential of formic acid generation reaction would be shifted to thermodynamic superiority over HER. Cations such as Na^+ and Li^+ were also found to have similar effect, but less significant compared with K^+.

2.5 Formic acid determination method

The determination of formic acid adopted the method proposed by Sleat et al. [48], which was based on a non-enzymatic specific reaction forming a red color with an absorption maximum at 510 nm when formate and several chemicals were mixed. During each set of experiment, exit electrolyte streams were collected after reaching steady state, 0.25 mL of which was extracted

and diluted by 0.25 mL deionized water as the sample. Meanwhile, 0.05 g citric acid was mixed with 1 g acetamide followed by ultrasonic dispersion in 10 mL 2-propanol. 0.5 mL of this mixture, together with 0.5 mL of the sample were dissolved in a mixture of 0.025mL 30% w/v sodium acetate and 1.75mL acetic anhydride for 1.5 hr. The absorbance of the solution mixture was obtained by a spectrophotometer (6105 U.V./Vis. Jenway) to determine the formate concentration. Calibration was conducted by quantitatively determining corresponding color formation in the presence of formate at 2.5, 5, 7.5, 10, 12.5, 15, 17.5 and 20 mmol/L, giving an correlative equation in Eq. 5.

$$0.0588 \times \text{Concentration of } \mathrm{HCOO^-} + 0.0562 = \text{Absorbance} \quad (5)$$

2.6 Efficiency calculation

Faradaic and energetic efficiencies are two key benchmarks for a CO_2 electrochemical reduction system. Faradaic efficiency indicates the fraction of the transferred electrons to facilitate the desired electrochemical reaction in a system. In this study, it is the formic acid formation reaction. Energetic efficiency is to measure the portion of energy converted and stored formic acid.

In order to calculate the Faradaic efficiency, we could obtain the total electrons passing through the reaction sites by measured current, then determine the electrons used for generating desired products based on the detected amount of formic acid. Denote the flow rate as M μL/min and the applied current to be N ampere. Assume that $\mathrm{HCOO^-}$ concentration is Y mol/L. The amount of detectable $\mathrm{HCOO^-}$ is $\mathrm{Y} \times \frac{\mathrm{M}}{10^6 \times 60}$ mol/s; hence, the amount of electrons transferred to produce formic acid is $2 \times \mathrm{Y} \times \frac{\mathrm{M}}{10^6 \times 60}$ mol/s. On the other hand, the number of electrons delivered to the electrode is $\mathrm{N} \times 1.04 \times 10^{-5}$ mol/s, giving Faradaic efficiency as shown in Eq. 6.

$$\mathrm{FE} = \frac{2 \times \mathrm{Y} \times \frac{\mathrm{M}}{10^6 \times 60}}{\mathrm{N} \times 1.04 \times 10^{-5}} \times 100\% \quad (6)$$

As for energetic efficiency, which considers voltage losses, the determination equation is defined in Eq. 7.

$$\text{Energetic efficiency} = \frac{\text{Standard potential}}{\text{Standard potential+Overpotential}} \times \text{Faradaic efficiency} \quad (7)$$

3. Results and discussion

3.1 Cathode catalyst selection

Pourbaix diagrams in Fig. 1 show the thermodynamic advantage of HER over formic acid generation. Experimentally, the applied cathode potentials for kinetically slow formic acid generation reaction, i.e. Reaction (1), would be from ~-0.8V to -1.8V with the overpotential from ~-0.4V to -1.4V[49], which is in the same potential range of HER, leading to selectivity decrease in aqueous electrolytes[13]. Thus, researchers have put efforts to select catalysts with high hydrogen overpotential to suppress HER, including Hg, In, Pb, and Sn[23, 50].

A DEMR was fabricated to construct a microchannel network, based on which different catalysts were tested for the comparison of key parameters such as current density, Faradaic efficiency and energy efficiency. Using the same electrolyte, i.e. 0.5 mol/L aqueous K_2SO_4 solution at pH=7, and anode material, i.e. commercially available PtRu (1:1 at.%) [51], cathode catalyst materials including palladium[52], tin[53], lead[10] and platinum series were tested for comparison.

Different current densities were applied to the reactor by varying the voltages to obtain the trends of reactivity and efficiencies. CO_2 concentration polarization would lead to lower Faradaic efficiency with increase in the applied voltage, so does the energetic efficiency because of the superposition of the elevated overpotentials. Nevertheless, there were dissents that on Sn[54] and

Pb at a CO_2 pressure of 5000 kPa(abs) [55], parabolic dependence of Faradaic efficiency on current density could be observed. These contradictions may be due to the rate determining step in the intrinsic kinetics of the formic acid generation reaction and should be addressed in a microfluidic reactor.

As shown in Fig. 3a, at a controlled voltage, PtIr showed the highest current densities, followed by PtRu, Pt black, and Pd. Sn catalyst demonstrated the highest current density below 3.5V and the smallest on-set electrolysis voltage. Pb showed the lowest current density. Microfluidics enables the investigation on the polarization of each electrodes as they were well separated by the virtual mixing layer. It could be observed that the ranking of whole cell performance conformed to that of the individual electrodes. The electrocatalytic activity toward CO_2 reduction could be further improved via tuning the morphology, electronic structure, and electrolysis conditions[56, 57], as the reactivity is highly dependent on the balance between the interactive strength (between $CO_2^{\cdot-}$ and the nanoscale metal surface) and the kinetics of following electronation and desorption from the electrode surface.

However, when looking at Faradaic efficiency, which indicates the portion of electrons used for producing formic acid, Pt-series catalysts, although with high catalytic reactivity, showed $<$ 35% Faradaic efficiency, i.e. low selectivity of converting CO_2 towards formic acid. This is due to the high water electrolysis catalytic rate and low hydrogen overpotential of Pt, favoring the HER[58, 59]. Although modifying the symmetry of the surface and introducing densely packed kink atoms along step lines would boost the activity for CO_2 reduction, the dominant reaction on Pt is to reduce CO_2 to CO[60], which might be adsorbed onto the catalyst surface, causing blockage.

Pb demonstrated a peak Faradaic efficiency as high as 80.5% at 2.8V, followed by Sn (73.2% at 3.5V) and Pd (62.4% at 3V). In terms of energetic efficiency, which takes voltage losses into consideration[61], Pb still showed superior performance up to 41% and surpassed other catalysts, implying its lower voltage loss. Selectivity is the key parameter to evaluate a CO_2 electrochemical reduction system and the purity of produced formic acid, and hence it should be considered prior to reactivity. Therefore, Pb was chosen as the cathode catalyst.

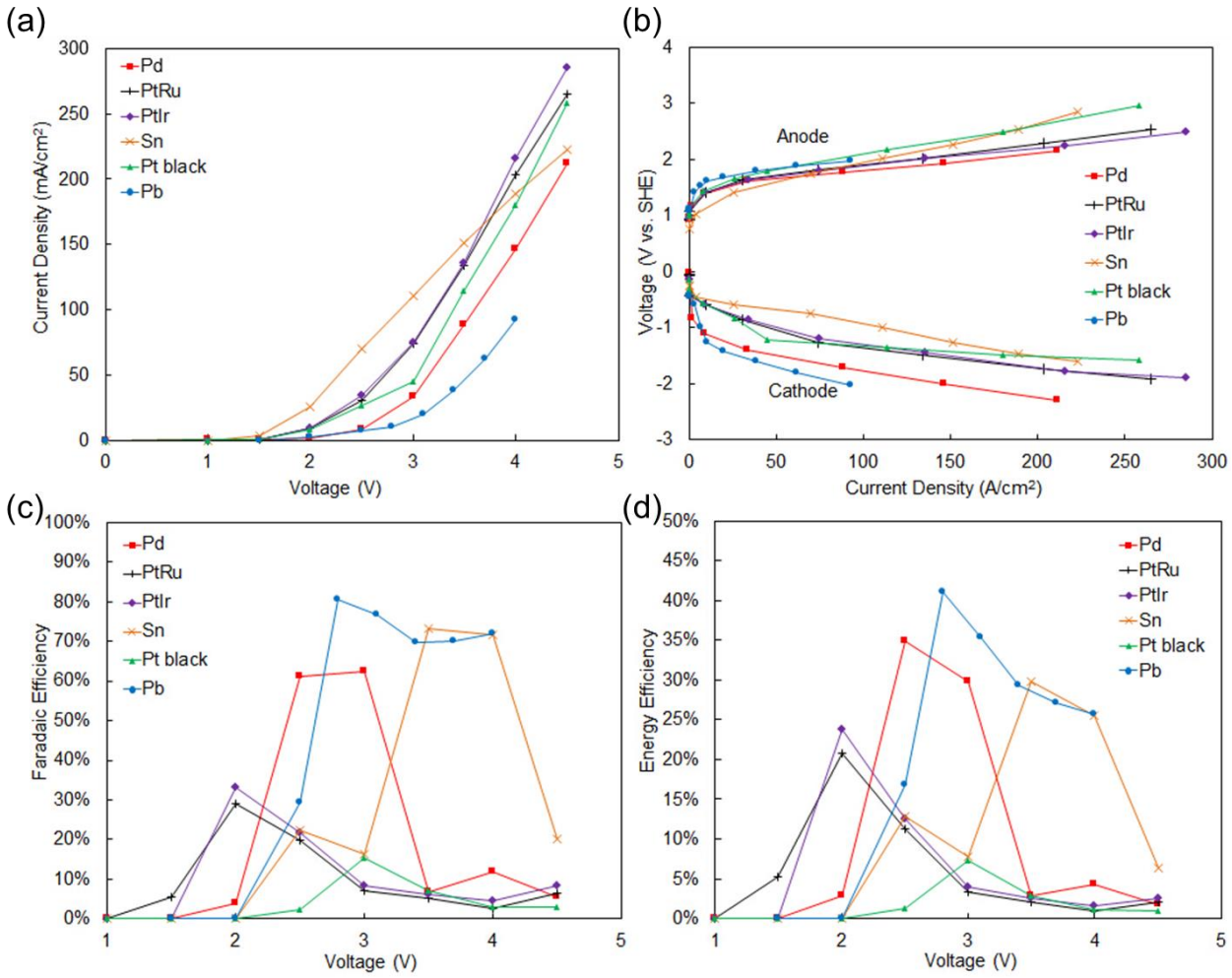

Fig. 3. (a) Polarization curves, (b) the corresponding individual electrode polarization curves, (c) Faradaic efficiencies, and (d) energetic efficiencies for cathode catalyst materials including Pd, PtRu, PtIr, Sn, Pt black and Pb. Anode catalyst material was PtRu. Both catholyte and anolyte were kept at pH=7 with a flow rate of 0.5 mL/min. CO_2 supply rate is 50 sccm.

3.2 Catholyte pH optimization

As previously explained, pH is an important factor that affects the performance of the DEMR. To identify the optimal catholyte pH, we applied the control variate method based on Pb cathode and PtRu anode combination. The anolyte pH was kept constant at pH=7, using common aqueous 0.5 mol/L K_2SO_4 solution, while the catholytes at different pHs were prepared by adjusting 0.5 mol/L K_2SO_4 with 0.5 mol/L H_2SO_4. This preparation process could help preclude the effect of conductivity and focus on pH. The reason to keep the conductivity constant is that a catholyte conductivity below 10 S/m would influence the applied reactor voltage and potential distribution in the electrode, which could be more significant with increasing the electrode thickness and current density[23]. To ensure a univariate analysis, sulfuric acid is used as the pH adjustor upon the potassium sulphate solution.

As can be seen in Fig. 4a, quantitated by current density, the whole cell reactivity at pH=0 catholyte was five times as much as that of pH=1, whose reactivity was more than twice as much as those of pH=2. The phenomenon corresponded to the fact that the concentration of H^+ dropped significantly from 1 mol/L to 0.1 mol/L. From pH=2 onwards, slight degradation of reactivity was observed because the absolute pH difference was less than 0.01 mol/L.

Fig. 4b gave a more detailed look into individual electrode performance. The individual anode polarization curves highly fitted with each other, whilst the cathode polarization curves followed the trend of the whole cell reactivity, i.e. cathode reactivity at pH=0 preceded pH=1 and stabilized from pH=2. The distinguished individual electrode reactivity validated the good utilization of microfluidic network by DEMR without significant mass transport loss.

In terms of efficiencies, no formic acid was detected in pH=0 and 1 due to the fact that hydrogen evolution reaction dominated at such high H^+ concentration and a large amount of

gaseous by-products could be observed during the reaction. The situation changed at pH=2, where a Faradaic efficiency of 90.8% and energetic efficiency of 46.4% was obtained at 2.8V. From pH=3 onwards, the figures were gradually diminishing, which was attributed to the drop in H^+ concentration. Considering both reactivity and efficiency, pH=2 gave the optimal overall performance and hence was selected as catholyte condition of our DEMR for further study.

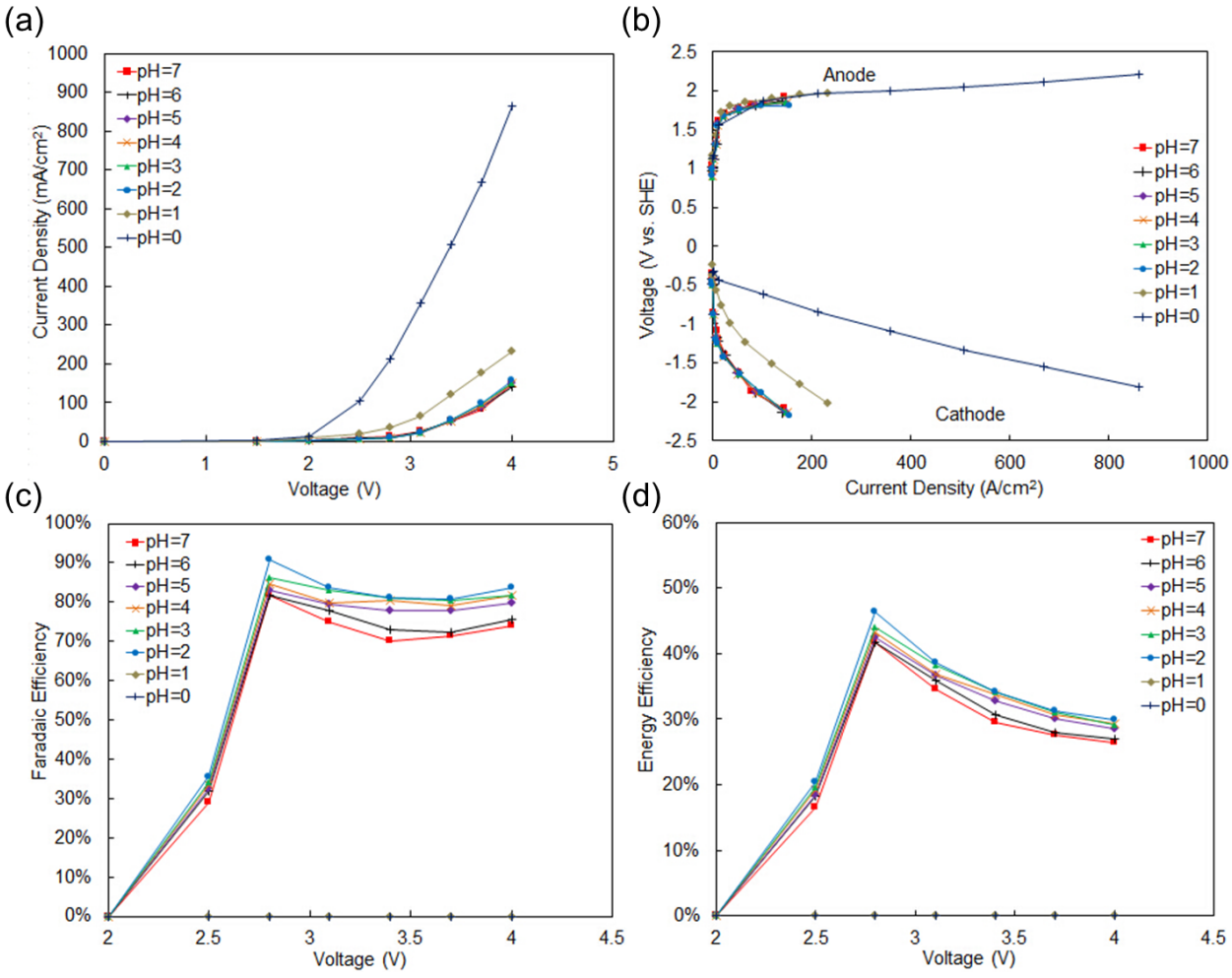

Fig. 4. (a) Polarization curves, (b) the corresponding individual electrode polarization curves, (c) Faradaic efficiencies, and (d) energetic efficiencies. Cathode catalyst material was Pb and anode was PtRu. Catholyte pH ranged from 7 to 0 and anolyte was kept at pH=7 with a flow rate of 0.5 mL/min. CO_2 supply rate is 50 sccm.

3.3 Anolyte pH optimization

With catholyte pH set to 2 (Section 3.2), the effect of anolyte pH was studied from pH=7 to pH=14, where the latter showed overwhelming advantage over others in terms of reactivity, i.e. four times more than pH=13 as quantitated by current density (Fig. 5a). Individual electrode polarization curves (Fig. 5b) demonstrated that pH=14 improved anode performance, which did not affect the cathode side and hence corroborating again that the microfluidics in our DEMR could effectively separate electrolytes and create distinguished conditions for electrodes.

Efficiencies were found in accordance with reactivity. When anolyte pH was 14, the peak Faradaic efficiency and energetic efficiency were as high as 95.6% and 48.5%, respectively. With decreasing pH, efficiencies dropped as indicated in Fig. 5c and 5d. It should be noted that increasing further the pH would lead to catalyst poisoning and instability. Thus, pH=14 was selected as anolyte pH for our DEMR.

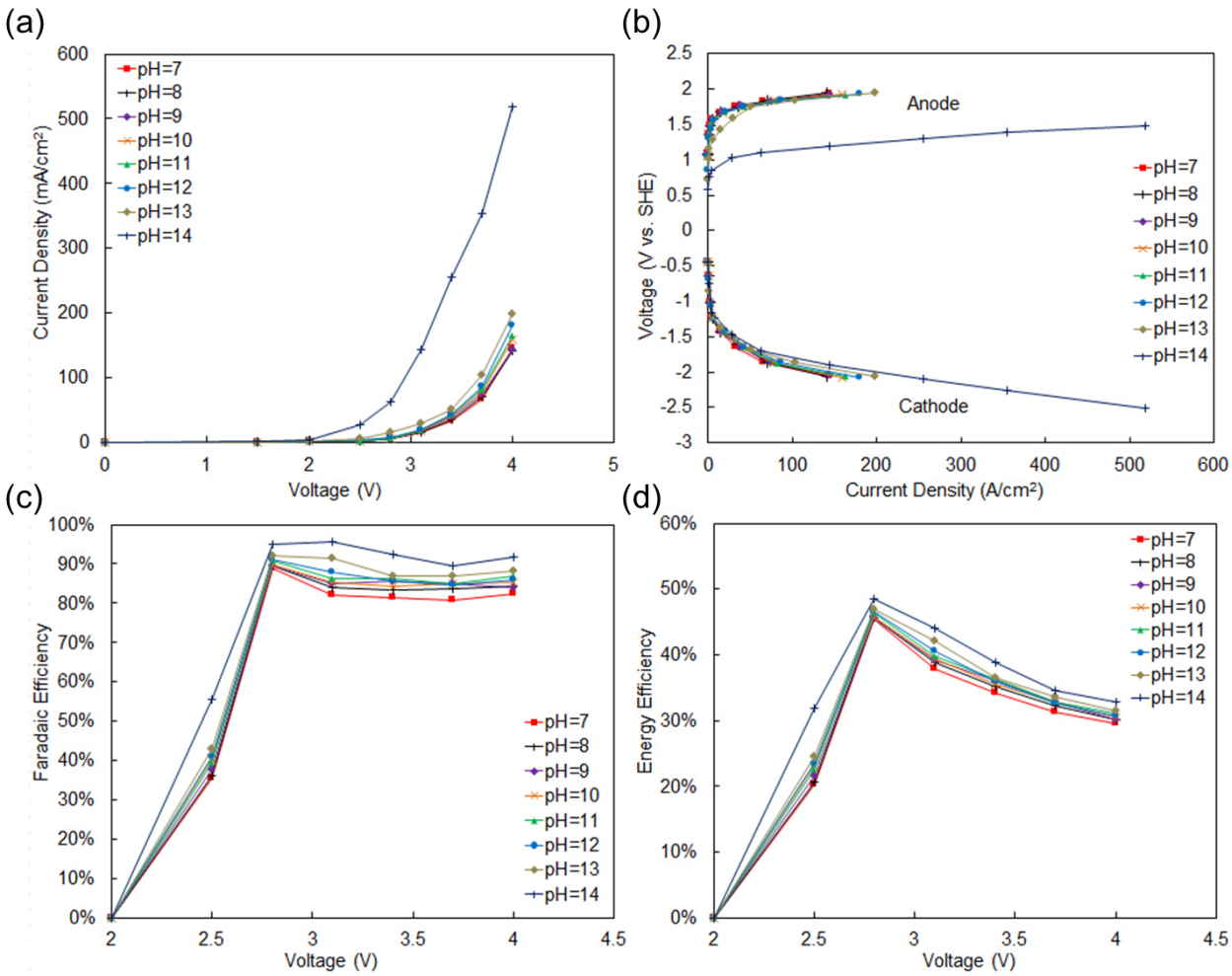

Fig. 5. (a) Polarization curves, (b) the corresponding individual electrode polarization curves, (c) Faradaic efficiencies, and (d) energetic efficiencies. Cathode catalyst material was Pb and anode was PtRu. Catholyte was kept at pH=2 and anolyte pH ranged from 7 to 14 with a flow rate of 0.5 mL/min. CO_2 supply rate is 50 sccm.

3.4 Optimization comparison and discussion

Fig. 6 summarizes the improvement introduced by the pH optimization. The current density remained almost unchanged after catholyte optimization because of the slight pH change; however, the current density was raised significantly from ~10 to ~60 mA/cm^2 after anolyte optimization, as can be seen in Fig. 6a. Fig. 6b demonstrates the thermodynamic improvement, where the cathode potential was reduced from -2.1V to -0.82V and the anode potential dropped

from 1.7V to 1V. Most importantly, Fig. 6c shows the increase of efficiencies, where electrolyte pH optimization raised the peak Faradaic efficiency from 81.6% to 95.6% and the peak energetic efficiency from 41.7% to 48.5%.

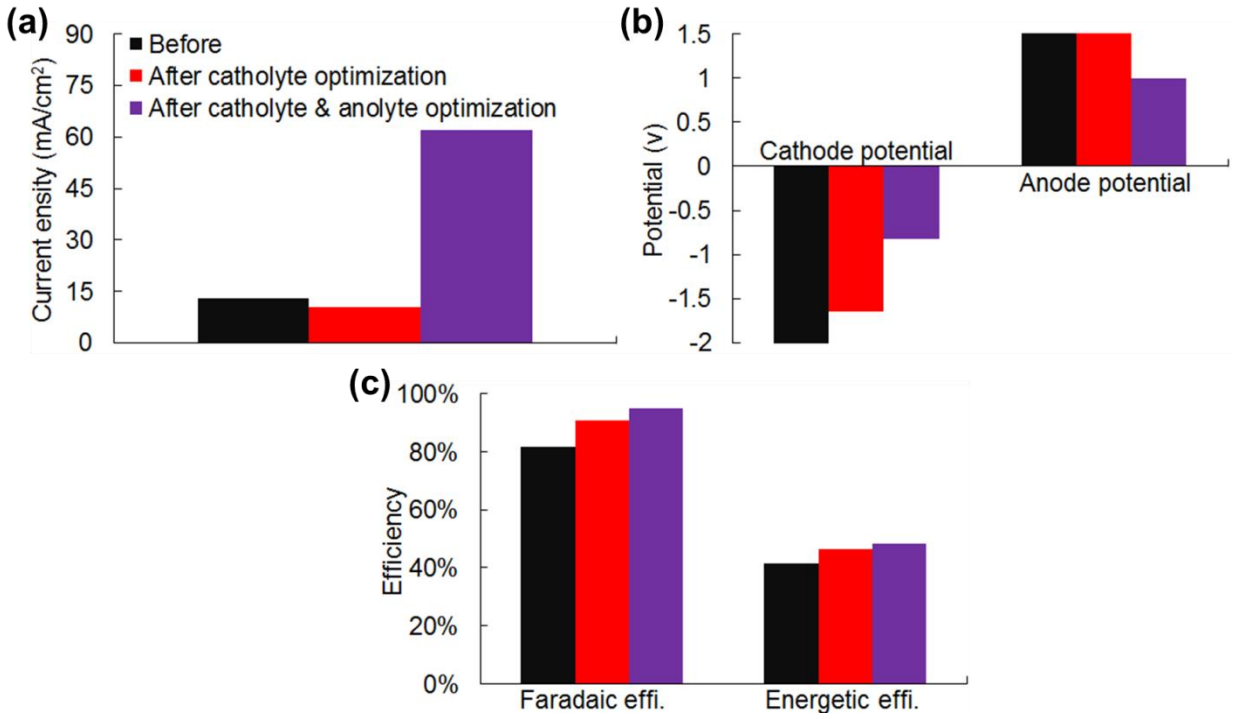

Fig. 6. (a) Current densities at an applied voltage of 2.8V, (b) cathode potentials at 100 mA/cm^2 under catholyte pHs of 7, 1 and 0; anode potentials at 150 mA/cm^2 under anolyte pHs of 7, 13 and 14, and (c) peak Faradaic and energetic efficiencies, before and after electrolyte optimization.

In theory, acid conditions on the cathode side and alkaline on the anode side can thermodynamically lower the potential difference. When applying acidic catholyte, a lower equilibrium potential of cathode reaction can be obtained (-0.199V in acid vs. -1.02V in alkaline, vs. NHE). More desired product, formic acid, can be generated with lower pH, especially when pH is less than 3[62], and hence increasing the Faradaic efficiency. Lower pH also favors the current density enhancement by reducing polarization losses, i.e. improves the reaction kinetics. It should be noted that unwanted HCO_3^- or HCO_3^{2-} could be generated under neutral or alkaline

conditions and the reactive CO_2(aq) would be sequestered as bicarbonate/carbonate at pH> 9. On the anode side, alkaline environment ensures the oxygen formation at low equilibrium potential.

A virtual separating layer between catholyte and anolyte can be observed in Fig. 2a. Heat visualization[63] showed that acid-base interfacial heat is dominant in a DEMR, whose ohmic Joule heat is much less than a single electrolyte system. Acid-base neutralization is known as a superfast reaction with a rate constant ~10^{11} M^{-1} s^{-1}[64] and might lead to significant losses without proper control method. This problem has been investigated and addressed by our previous study[63], where the fluorescence microscopy was utilized to demonstrate that raising the flow rate (e.g. 1.4 mL/min) could enhance the heat removal and formed a thinner interfacial mixing layer, hence controlling the reactor temperature and suppressing the heat loss.

Despite the fact that a microfluidic network can shorten the path required for ions diffusion in the narrow channel[65], the solubility of CO_2 is rather low in aqueous electrolytes, limiting its mass transfer to the reaction site. Microfluidics properties in our DEMR can be enhanced by fully utilizing the large interfacial areas and effective three-phase interface (i.e. gaseous CO_2, solid catalyst, and liquid electrolyte) in gas diffusion electrodes[66]. Also, pH adjustment can be applied on other electrolytes with high CO_2 solubility and HER overpotential, such as organic electrolytes[18] [19, 20] and ionic liquids[67-69], to improve the whole cell performance.

4. Conclusions

This work demonstrates the possibility of advancing CO_2 electrochemical reduction via thermodynamic approach based on microfluidics. Different catalysts favoured CO_2 electro-conversion into formic acid to various extents. By comparing six commonly used noble metal

catalysts, the combination of Pb cathode and PtRu anode was found to give the highest efficiencies despite of its relatively low catalytic activity. The merit comes from the fact that Pb has higher overpotentials for HER[10] and Pt is an active oxygen evolution catalyst. This study is the first systematic investigation to apply pH differential technique on CO_2 reduction, concluding that catholyte pH=2 and anolyte pH=14 output the optimal cell performance. In a dual electrolyte system, the reactivity was tripled than a single neutral electrolyte arrangement and the peak Faradaic efficiency was improved from 81.6% to 95.6%. In conclusion, this design not only provides a solution towards the improvement of current CO_2 utilization system, but also serves as a potential powerful and efficient energy storage platform.

Acknowledgement

This project is financially supported by the CRCG of the University of Hong Kong and the Scottish – Hong Kong SFC/RGC Joint Research Scheme XHKU710/14 and SFC Project H15009.

References

[1] J. Qiao, Y. Liu, F. Hong, J. Zhang, A review of catalysts for the electroreduction of carbon dioxide to produce low-carbon fuels, Chemical Society Reviews, 43 (2014) 631-675.
[2] J.P. Jones, G. Prakash, G.A. Olah, Electrochemical CO2 reduction: recent advances and current trends, Israel Journal of Chemistry, 54 (2014) 1451-1466.
[3] E.E. Benson, C.P. Kubiak, A.J. Sathrum, J.M. Smieja, Electrocatalytic and homogeneous approaches to conversion of CO 2 to liquid fuels, Chemical Society Reviews, 38 (2009) 89-99.
[4] A.J. Martín, G.O. Larrazábal, J. Pérez-Ramírez, Towards sustainable fuels and chemicals through the electrochemical reduction of CO 2: lessons from water electrolysis, Green Chemistry, 17 (2015) 5114-5130.
[5] S. Park, J.-W. Lee, B.N. Popov, A review of gas diffusion layer in PEM fuel cells: materials and designs, international journal of hydrogen energy, 37 (2012) 5850-5865.
[6] Y. Hori, H. Wakebe, T. Tsukamoto, O. Koga, Electrocatalytic process of CO selectivity in electrochemical reduction of CO2 at metal electrodes in aqueous media, Electrochimica Acta, 39 (1994) 1833-1839.

[7] C. Simon, F. Hasché, D. Müller, H.A. Gasteiger, Influence of the Gas Diffusion Layer Compression on the Oxygen Mass Transport in PEM Fuel Cells, ECS Transactions, 69 (2015) 1293-1302.
[8] G. Lu, H. Wang, Z.-Y. Bian, X. Liu, Electrocatalytic Reduction of CO2 to Formic Acid on Palladium-Graphene Nanocomposites Gas-Diffusion Electrode, Journal of nanoscience and nanotechnology, 14 (2014) 7097-7103.
[9] H.-R.M. Jhong, S. Ma, P.J.A. Kenis, Electrochemical conversion of CO2 to useful chemicals: current status, remaining challenges, and future opportunities, Current Opinion in Chemical Engineering, 2 (2013) 191-199.
[10] C.H. Lee, M.W. Kanan, Controlling H+ vs CO2 reduction selectivity on Pb electrodes, ACS Catalysis, 5 (2014) 465-469.
[11] N. Furuya, T. Yamazaki, M. Shibata, High performance Ru-Pd catalysts for CO2 reduction at gas-diffusion electrodes, Journal of Electroanalytical Chemistry, 431 (1997) 39-41.
[12] M.N. Mahmood, D. Masheder, C.J. Harty, Use of gas-diffusion electrodes for high-rate electrochemical reduction of carbon dioxide. II. Reduction at metal phthalocyanine-impregnated electrodes, Journal of Applied Electrochemistry, 17 (1987) 1223-1227.
[13] D. Kopljar, A. Inan, P. Vindayer, N. Wagner, E. Klemm, Electrochemical reduction of CO2 to formate at high current density using gas diffusion electrodes, Journal of Applied Electrochemistry, 44 (2014) 1107-1116.
[14] M. Alvarez-Guerra, J. Albo, E. Alvarez-Guerra, A. Irabien, Ionic liquids in the electrochemical valorisation of CO 2, Energy & Environmental Science, 8 (2015) 2574-2599.
[15] D.R. MacFarlane, N. Tachikawa, M. Forsyth, J.M. Pringle, P.C. Howlett, G.D. Elliott, J.H. Davis, M. Watanabe, P. Simon, C.A. Angell, Energy applications of ionic liquids, Energy & Environmental Science, 7 (2014) 232-250.
[16] Z. Zhang, S. Hu, J. Song, W. Li, G. Yang, B. Han, Hydrogenation of CO2 to Formic Acid Promoted by a Diamine-Functionalized Ionic Liquid, ChemSusChem, 2 (2009) 234-238.
[17] M.R. Thorson, K.I. Siil, P.J. Kenis, Effect of Cations on the Electrochemical Conversion of CO2 to CO, Journal of the Electrochemical Society, 160 (2013) F69-F74.
[18] E. Rischbieter, A. Schumpe, V. Wunder, Gas solubilities in aqueous solutions of organic substances, Journal of Chemical & Engineering Data, 41 (1996) 809-812.
[19] D.-w. Yang, Q.-y. Li, F.-x. Shen, Q. Wang, L. Li, N. Song, Y.-n. Dai, J. Shi, Electrochemical Impedance Studies of CO 2 Reduction in Ionic Liquid/Organic Solvent Electrolyte on Au Electrode, Electrochimica Acta, 189 (2016) 32-37.
[20] R. Kortlever, J. Shen, K.J.P. Schouten, F. Calle-Vallejo, M.T. Koper, Catalysts and Reaction Pathways for the Electrochemical Reduction of Carbon Dioxide, The journal of physical chemistry letters, 6 (2015) 4073-4082.
[21] J.L. Cohen, D.J. Volpe, D.A. Westly, A. Pechenik, H.D. Abruña, A dual electrolyte H2/O2 planar membraneless microchannel fuel cell system with open circuit potentials in excess of 1.4 V, Langmuir, 21 (2005) 3544-3550.
[22] S. Cheng, K.-Y. Chan, High-Voltage Dual Electrolyte Electrochemical Power Sources, ECS Transactions, 25 (2010) 213-219.
[23] H. Li, C. Oloman, Development of a continuous reactor for the electro-reduction of carbon dioxide to formate–Part 1: Process variables, Journal of Applied Electrochemistry, 36 (2006) 1105-1115.
[24] H. Li, C. Oloman, The Electro-Reduction of Carbon Dioxide in a Continuous Reactor, Journal of Applied Electrochemistry, 35 (2005) 955-965.

[25] F. Köleli, T. Atilan, N. Palamut, A.M. Gizir, R. Aydin, C.H. Hamann, Electrochemical reduction of CO2 at Pb- and Sn-electrodes in a fixed-bed reactor in aqueous K2CO3 and KHCO3 media, Journal of Applied Electrochemistry, 33 (2003) 447-450.
[26] H. Zhang, M.K.H. Leung, J. Xuan, H. Xu, L. Zhang, D.Y.C. Leung, H. Wang, Energy and exergy analysis of microfluidic fuel cell, International Journal of Hydrogen Energy, 38 (2013) 6526-6536.
[27] H. Wang, D.Y.C. Leung, J. Xuan, Modeling of a micro auto-electrolytic cell for hydrogen production, International Journal of Hydrogen Energy, 37 (2012) 10009.
[28] K. Hsieh, A.S. Patterson, B.S. Ferguson, K.W. Plaxco, H.T. Soh, Rapid, Sensitive, and Quantitative Detection of Pathogenic DNA at the Point of Care through Microfluidic Electrochemical Quantitative Loop-Mediated Isothermal Amplification, Angewandte Chemie, 124 (2012) 4980-4984.
[29] Y. Wu, P. Xue, K.M. Hui, Y. Kang, A paper-based microfluidic electrochemical immunodevice integrated with amplification-by-polymerization for the ultrasensitive multiplexed detection of cancer biomarkers, Biosensors and Bioelectronics, 52 (2014) 180-187.
[30] G.P. Roth, R. Stalder, T.R. Long, D.R. Sauer, S.W. Djuric, Continuous-flow microfluidic electrochemical synthesis: investigating a new tool for oxidative chemistry, Journal of Flow Chemistry, 3 (2013) 34-40.
[31] S. Sabatino, A. Galia, O. Scialdone, Electrochemical Abatement of Organic Pollutants in Continuous-Reaction Systems through the Assembly of Microfluidic Cells in Series, ChemElectroChem, 3 (2016) 83-90.
[32] D. Voicu, M. Abolhasani, R. Choueiri, G. Lestari, C. Seiler, G. Menard, J. Greener, A. Guenther, D.W. Stephan, E. Kumacheva, Microfluidic studies of CO2 sequestration by frustrated Lewis pairs, Journal of the American Chemical Society, 136 (2014) 3875-3880.
[33] H. Wang, D.Y.C. Leung, J. Xuan, Modeling of a microfluidic electrochemical cell for CO2 utilization and fuel production, Applied Energy, 102 (2013) 1057-1062.
[34] M. Abolhasani, A. Günther, E. Kumacheva, Microfluidic studies of carbon dioxide, Angewandte Chemie International Edition, 53 (2014) 7992-8002.
[35] K. Wu, E. Birgersson, B. Kim, P.J. Kenis, I.A. Karimi, Erratum: Modeling and Experimental Validation of Electrochemical Reduction of CO2 to CO in a Microfluidic Cell [J. Electrochem. Soc., 162, F23 (2015)], Journal of The Electrochemical Society, 162 (2015) X6-X6.
[36] D.T. Whipple, E.C. Finke, P.J.A. Kenis, Microfluidic reactor for the electrochemical reduction of carbon dioxide: The effect of pH, Electrochemical and Solid-State Letters, 13 (2010) B109-B111.
[37] E.R. Choban, J.S. Spendelow, L. Gancs, A. Wieckowski, P.J.A. Kenis, Membraneless laminar flow-based micro fuel cells operating in alkaline, acidic, and acidic/alkaline media, Electrochimica Acta, 50 (2005) 5390-5398.
[38] A. Boddien, D. Mellmann, F. Gärtner, R. Jackstell, H. Junge, P.J. Dyson, G. Laurenczy, R. Ludwig, M. Beller, Efficient dehydrogenation of formic acid using an iron catalyst, Science, 333 (2011) 1733-1736.
[39] C. Rice, S. Ha, R.I. Masel, P. Waszczuk, A. Wieckowski, T. Barnard, Direct formic acid fuel cells, Journal of Power Sources, 111 (2002) 83-89.
[40] X. Yu, P.G. Pickup, Recent advances in direct formic acid fuel cells (DFAFC), Journal of Power Sources, 182 (2008) 124-132.

[41] N. Sridhar, D. Hill, Carbon dioxide utilization Electrochemical conversion of CO_2 – Opportunities and Challenges, in: Research and Innovation, Position Paper, Det Norske vertas, Høvik, Norway, 2011.
[42] A.S. Agarwal, Y. Zhai, D. Hill, N. Sridhar, The electrochemical reduction of carbon dioxide to formate/formic acid: Engineering and economic feasibility, ChemSusChem, 4 (2011) 1301-1310.
[43] T. Reda, C.M. Plugge, N.J. Abram, J. Hirst, Reversible interconversion of carbon dioxide and formate by an electroactive enzyme, Proceedings of the National Academy of Sciences, 105 (2008) 10654-10658.
[44] S.K. Lower, Acid-base equilibria and calculations, in, A Chem, 2014.
[45] Y. Hori, S. Suzuki, Electrolytic reduction of carbon dioxide at mercury electrode in aqueous solution, Bulletin of the Chemical Society of Japan, 55 (1982) 660-665.
[46] C. Sanchez-Sanchez, V. Montiel, D. Tryk, A. Aldaz, A. Fujishima, Electrochemical approaches to alleviation of the problem of carbon dioxide accumulation, Pure and Applied Chemistry, 73 (2001) 1917-1927.
[47] N. Gupta, M. Gattrell, B. MacDougall, Calculation for the cathode surface concentrations in the electrochemical reduction of CO2 in KHCO3 solutions, Journal of Applied Electrochemistry, 36 (2006) 161-172.
[48] R. Sleat, R.A. Mah, Quantitative method for colorimetric determination of formate in fermentation media, Applied and environmental microbiology, 47 (1984) 884.
[49] H. Li, C. Oloman, Development of a continuous reactor for the electro-reduction of carbon dioxide to formate – Part 2: Scale-up, Journal of Applied Electrochemistry, 37 (2007) 1107-1117.
[50] X. Lu, D.Y. Leung, H. Wang, M.K. Leung, J. Xuan, Electrochemical reduction of carbon dioxide to formic acid, ChemElectroChem, 1 (2014) 836-849.
[51] T. Reier, M. Oezaslan, P. Strasser, Electrocatalytic oxygen evolution reaction (OER) on Ru, Ir, and Pt catalysts: a comparative study of nanoparticles and bulk materials, Acs Catalysis, 2 (2012) 1765-1772.
[52] X. Min, M.W. Kanan, Pd-catalyzed electrohydrogenation of carbon dioxide to formate: High mass activity at low overpotential and identification of the deactivation pathway, Journal of the American Chemical Society, 137 (2015) 4701-4708.
[53] A. Del Castillo, M. Alvarez-Guerra, J. Solla-Gullón, A. Sáez, V. Montiel, A. Irabien, Electrocatalytic reduction of CO 2 to formate using particulate Sn electrodes: Effect of metal loading and particle size, Applied Energy, 157 (2015) 165-173.
[54] T.M.a.S.I. K. Ito, Electrochemical reduction of carbon dioxide on zinc and cadmium electrodes, Zh. Prikl. Khim., Bulletin of the Nagoya Institute of Technology, 209-214 (1975).
[55] F. Köleli, D. Balun, Reduction of CO 2 under high pressure and high temperature on Pb-granule electrodes in a fixed-bed reactor in aqueous medium, Applied Catalysis A: General, 274 (2004) 237-242.
[56] Y. Chen, M.W. Kanan, Tin oxide dependence of the CO2 reduction efficiency on tin electrodes and enhanced activity for tin/tin oxide thin-film catalysts, Journal of the American Chemical Society, 134 (2012) 1986-1989.
[57] J. Wu, F.G. Risalvato, F.-S. Ke, P. Pellechia, X.-D. Zhou, Electrochemical reduction of carbon dioxide I. Effects of the electrolyte on the selectivity and activity with Sn electrode, Journal of The Electrochemical Society, 159 (2012) F353-F359.

[58] S. Grigoriev, P. Millet, V. Fateev, Evaluation of carbon-supported Pt and Pd nanoparticles for the hydrogen evolution reaction in PEM water electrolysers, Journal of Power Sources, 177 (2008) 281-285.
[59] M. Carmo, D.L. Fritz, J. Mergel, D. Stolten, A comprehensive review on PEM water electrolysis, International Journal of Hydrogen Energy, 38 (2013) 4901-4934.
[60] Y. Hori, H. Wakebe, T. Tsukamoto, O. Koga, Electrocatalytic process of CO selectivity in electrochemical reduction of CO 2 at metal electrodes in aqueous media, Electrochimica Acta, 39 (1994) 1833-1839.
[61] R. Williams, R.S. Crandall, A. Bloom, Use of carbon dioxide in energy storage, Applied Physics Letters, 33 (1978) 381-383.
[62] C. Oloman, H. Li, Electrochemical processing of carbon dioxide, Chemsuschem, 1 (2008) 385-391.
[63] Lu X, Xuan J, Leung DYC, Zou HY, Li JT, Wang HL, a.W. HZ, A switchable pH-differential unitized regenerative fuel cell with high power density and round-trip efficiency, Journal of Power Sources, 314 (2016) 76-84.
[64] S. Druckmann, M. Ottolenghi, A. Pande, J. Pande, R. Callender, Acid-base equilibrium of the Schiff base in bacteriorhodopsin, Biochemistry, 21 (1982) 4953-4959.
[65] J. Kobayashi, Y. Mori, K. Okamoto, R. Akiyama, M. Ueno, T. Kitamori, S. Kobayashi, A microfluidic device for conducting gas-liquid-solid hydrogenation reactions, Science, 304 (2004) 1305-1308.
[66] D.T. Whipple, P.J.A. Kenis, Prospects of CO2 Utilization via Direct Heterogeneous Electrochemical Reduction, The Journal of Physical Chemistry Letters, 1 (2010) 3451-3458.
[67] X. Huang, C.J. Margulis, Y. Li, B.J. Berne, Why is the partial molar volume of CO2 so small when dissolved in a room temperature ionic liquid? Structure and dynamics of CO2 dissolved in [Bmim+][PF6-], Journal of the American Chemical Society, 127 (2005) 17842-17851.
[68] Á. Pérez-Salado Kamps, D. Tuma, J. Xia, G. Maurer, Solubility of CO2 in the ionic liquid [bmim][PF6], Journal of Chemical & Engineering Data, 48 (2003) 746-749.
[69] J. Kumelan, Á.P.-S. Kamps, D. Tuma, G. Maurer, Solubility of CO2 in the ionic liquids [bmim][CH3SO4] and [bmim][PF6], Journal of Chemical & Engineering Data, 51 (2006) 1802-1807.